Visualization of 2D Scalar Field Ensembles Using Volume Visualization of the Empirical Distribution Function

Tomas Daetz* Leipzig University
Michael Böttinger† German Climate Computing Center
Gerik Scheuermann‡ Leipzig University
Christian Heine§ Leipzig University

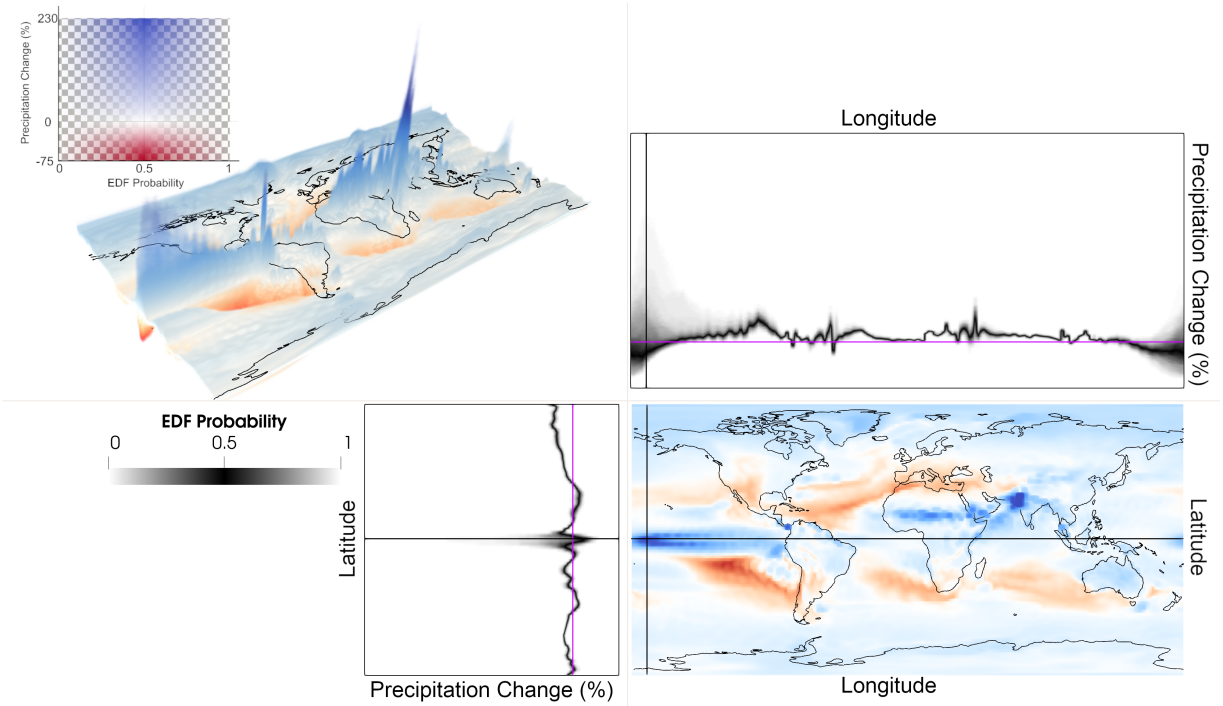

Figure 1: Precipitation change (%) in 2080-2099 relative to 1986-2005 based on 100 simulation runs of the RCP8.5 scenario within MPI-GE. The top left panel shows a volume rendering of the cumulative height field using a 2D transfer function, mapping cumulative probabilities to opacity and precipitation change to color (blue: increase, red: decrease), and an isosurface of the median. The bottom right panel shows an orthographic view of the same scene. The black lines indicate the locations of the cumulative function graphs at 0° and 170°W, which are shown in the top right and bottom left panels, respectively. The purple lines depict zero percent difference. The intersection of the black lines mark the chosen point of interest (0°, 170°W), where the distribution is skewed: while most ensemble members show a small to moderate decrease in precipitation, a few outliers show a large increase, which means that the arithmetic mean at this point would indicate an - though unlikely - increase in precipitation.

Abstract

Analyzing uncertainty in spatial data is a vital task in many domains, as for example with climate and weather simulation ensembles. Although many methods support the analysis of uncertain 2D data, such as uncertain isocontours or overlaying of statistical information on plots of the actual data, it is still a challenge to get a more detailed overview of 2D data together with its statistical properties. We present *cumulative height fields*, a visualization method for 2D scalar field ensembles using the *marginal empirical distribution function* and show preliminary results using volume rendering and slicing for the Max Planck Institute Grand Ensemble.

Index Terms: Scalar field visualization, ensemble visualization, volume rendering, nonparametric statistics.

*e-mail: daetz@informatik.uni-leipzig.de
†e-mail: boettinger@dkrz.de
‡e-mail: scheuermann@informatik.uni-leipzig.de
§e-mail: heine@informatik.uni-leipzig.de

1 Introduction

In the natural sciences, uncertainty is generally an essential component in observed or simulated data. Analyzing data together with their respective uncertainties is needed to estimate the robustness of results and to make statements about the probabilities of certain events. A typical question in climate research, for example, is how likely it is that flooding caused by heavy rainfall will occur more frequently in a particular region in the future.

There are many methods to investigate and visualize uncertainty in data. For 2D scalar fields, these include spaghetti plots, contour boxplots [32], estimating distributions parameters, e.g. mean and standard deviation, or calculating summary statistics, e.g. median and percentiles. But not all distributions are simple enough to be summarized by a single measure, e.g. highly skewed or multimodal distributions. Such features in the distribution can affect the interpretation by domain experts, but might be missed when using summary statistics or assuming an underlying distribution a priori. A direct visual analysis of the distribution, which is often unknown and must first be estimated, is not necessarily straightforward. Although a distribution can be easily visualized for the 1D case, it is rather difficult to visualize in the case of (higher dimensional) scalar fields. In this paper, we propose the combination of empir-

ical distribution functions with volume visualization to study the distribution of 2D scalar field ensembles.

Our main contributions are: (1) A visualization of the marginal empirical distribution functions, the *cumulative height fields*, for 2D scalar field ensembles, combining direct volume rendering, which gives an overview of the data and its variability, with volume slicing for details, and (2) Preliminary results of applying the technique to study changes in precipitation in simulations of climate change.

2 Related Work

A state-of-the-art in visualizing uncertain scalar fields and a survey of visualization in meteorology were presented by Wang et al. [30] and Rautenhaus et al. [25], respectively. A typical approach often used in the domain sciences is to visualize the mean of some uncertain quantity and to calculate and display its standard deviation as an overlay, as done by Potter et al. [20], where mean and standard deviation were used to draw isolines and colormap the domain. Sanyal et al. [27] used various uncertainty glyphs and ribbons based on different uncertainty metrics.

A fundamental technique for isocontours of uncertain data are the level crossing probabilities (LCP), introduced by Pöthkow and Hege [21], where the probability of isocontours for a given isovalue to cross a cell is calculated for all cells in the domain. The LCPs can then be visualized by colormapping for the 2D or volume rendering for the 3D case. There have been several extensions to the LCPs [22, 24, 23, 12]. Allendes Osorio and Brodlie [3] presented a definition of isocontour bands of points with a higher probability of having an isocontour and Pfaffelmoser et al. [18] use a ray-casting technique to calculate uncertain isosurfaces considering correlations. Athawale and Entezari [4] introduced the closed-form expression for the expected crossing of isocontours with the assumption of an underlying uniform distribution. Athawale et al. [5] expanded this to allow for nonparametric distributions using kernel density estimates. The expected crossings can then be colored using the calculated variance. A drawback is that here the distribution in the data is again reduced to an expected value and a variance.

Many methods show the information in a *boxplot* style, i.e. a representation of median, mean, some confidence regions and outliers, which have been adopted for different data: 1D [29] and 2D [11] scalar field ensembles, ensembles of parametrized curves [17] and the contour boxplots for isoline ensembles [32], each method based on some extension of the concept of *band depth*. More recently, Chaves-de-Plaza et al. [8] presented another depth concept to use for contour boxplots, and further expanded it to support multimodal isocontour ensembles [7]. Other summarization methods have been presented as well [10, 15, 33]. All these approaches require the domain expert to provide an isovalue, but do not provide means to indicate which isovalues might be interesting.

There has been work on using direct volume rendering (DVR) to include the uncertainty information, such as the one by Djurcilov et al. [9], who present 2D transfer functions that use scalar values and uncertainties to map optical properties. Sakhaee and Entezari [26] developed a histogram-based volume rendering approach that uses transfer functions for the deterministic case, and Athawale et al. [6] also present a nonparametric approach based on quantile interpolation and provide the quartile view, which shows three different plots for the bottom 25%, the middle 50% and the top 25% of the data, similar to the information in a boxplot. But as these works are volume rendering methods of uncertain 3D scalar fields, they are not directly applicable to the visualization of uncertain 2D scalar fields or the visualization of the marginal distributions.

Most related to our work for the visualization of uncertain 2D scalar fields is the visualization presented by Pfaffelmoser and Westermann [19], who visualize the mean field as a height field with inserted glyphs, depicting information of points clustered by correlation and the variance of the marginal distributions. Further, Kao et al. [14] present various visualizations for 2D scalar field ensembles based on statistical moments, but also extend the 2D domain to 3D and fill the volume with the values of the marginal probability density function (PDF) of each point. Different visualizations were presented using this volume, like cutting planes, and although DVR was briefly described, it was not used. Höllt et al. [13] presented within their framework a visualization of the volume of marginal PDF values as a colormapped volume for a given region of interest.

3 Background

Our method makes use of standard concepts in probability theory [31]. Let $(\Omega, \mathscr{F}, \mathbb{P})$ be a probability space, where Ω is the sample space, $\mathscr{F}$ a σ-algebra over Ω and $\mathbb{P}$ the probability measure. A *random variable* Y is a mapping $Y : \Omega \to \mathbb{R}$, and the *cumulative distribution function (CDF)* is the function $F_Y : \mathbb{R} \to [0,1]$ defined by $F_Y(y) = \mathbb{P}(Y \leq y)$. We write $Y \sim F_Y$ and assume all random variables to be continuous. Under this condition, the *probability density function (PDF)* can be defined as $f_Y(y) = \frac{\mathrm{d}F_Y}{\mathrm{d}y}(y)$. A *random vector* $Y : \Omega \to \mathbb{R}^n, Y = (Y_1, \ldots, Y_n)$ is a set of random variables, with associated joint CDF $F_Y(y_1, \ldots, y_n) = \mathbb{P}(Y_1 \leq y_1, \ldots, Y_n \leq y_n)$ and joint PDF $f_Y(y_1, \ldots, y_n)$. *Marginalizing* a random variable from a set of random variables means to determine its distribution from the joint distribution over the random variables, e.g. marginalizing for Y_1 is $f_{Y_1}(y) = \int_{-\infty}^{\infty} \cdots \int_{-\infty}^{\infty} f_Y(y, y_2, \ldots, y_n)\, \mathrm{d}y_2 \cdots \mathrm{d}y_n$. A set of random variables are *independent*, if their joint PDF equals the product of their marginal PDFs everywhere, i.e. if $f_Y(y_1, \ldots, y_n) = \prod_{i=1}^{n} f_{Y_i}(y_i)$ holds.

Often the distribution of a random variable is not known, but can be approximated. Let $Y_1, \ldots, Y_k$ be independent random variables with the same distribution $Y_i \sim F$, then the *empirical distribution function (EDF)* is defined as $\hat{F}(\theta) = \frac{1}{k} \sum_{i=1}^{k} \mathbb{1}_{(-\infty, \theta]}(Y_i)$, where $\mathbb{1}_{(-\infty, \theta]}(y) = 1$ if $y \leq \theta$ and 0 otherwise. The EDF forms a staircase function, taking value 0 and 1 for all the points below the sample minimum and above the sample maximum, respectively. As $k \to \infty$ the EDF converges on the CDF F.

A deterministic scalar field is a function $f : D \to \mathbb{R}$. In practice, the data describing the scalar field are given as a set of values $(y_1, \ldots, y_n)$ at grid points $G = \{\mathbf{x}_1, ..., \mathbf{x}_n\} \subseteq D$ and use interpolation between grid points. Although an uncertain scalar field can be modeled as a *random field* [1], the typical model used are random vectors, where each sample point $\mathbf{x}_i \in G, i \in \{1, ..., n\}$ gets assigned to a random variable Y_i, forming the random vector $Y = (Y_1, ..., Y_n)$. To simplify the notation throughout this paper, $\mathbf{x}_i$ will always refer to some arbitrary point in G, while Y_i refers to the respective random variable of $\mathbf{x}_i$. In practice, instead of a distribution, only samples from the uncertain scalar field $f_1, ..., f_k$ are available, where each f_i is itself a scalar field with function values only defined on G.

4 Cumulative Function Graphs (CFG) & Cumulative Height Fields (CHF)

4.1 Theory & Construction

Our method is motivated by the desire to look at the (estimated) distribution of members of an ensemble in order to emphasize distribution properties that might be missed in summary statistics, e.g. multimodality. While univariate random variables' distributions can be depicted by a line graph of their CDF or PDF, visualizing the distribution of multivariate random variables is more challenging, due to the possible statistical dependency among variables. Additionally, Silverman [28] notes that in order to estimate the distribution of a multivariate random variable, one needs asymptotically a number of samples exponential in the number of variables. Since we assign each grid point a random variable and grids typically comprise many grid points, estimating the full multivariate distribution is impractical. Instead, we estimate the marginal CDF via the EDF for

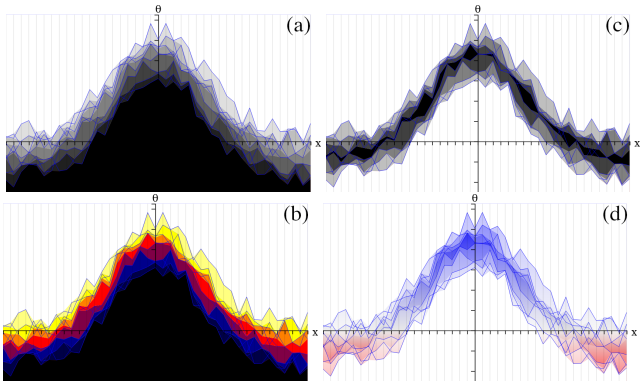

Figure 2: Illustration of cumulative function graph colormapped with different color scales. The blue lines are the function graphs for each of the original ensemble members. In (a), the cumulative probability is mapped linearly to lightness. In (b), a black body radiation color map is used. In (c), the color scale goes from white to black to white again, emphasizing the central percentiles. In (d), a 2D color scale is used: the function value θ is mapped to a red-white-blue color scale and the cumulative probability is mapped to opacity, emphasizing values above and below a function value of interest.

each grid point, which is accurate but loses all information about statistical dependencies between grid points.

As the marginal EDF is a function for each grid point, it is necessary to expand the original domain with the codomain for the visualization. This is rather similar to line graphs for 1D and height fields for 2D functions, where the codomain dimension is used to show where the function value is, allowing for an overview of the function's form. For uncertain scalar fields, the function value at $\mathbf{x}_i$ is not known, but instead we can calculate $\mathbb{P}(Y_i \leq \theta)$ for any $\theta \in \mathbb{R}$. Then, we can turn an uncertain d-dimensional scalar field into a $d+1$-dimensional scalar field $\overline{f} : D \times \mathbb{R} \rightarrow [0,1]$ with $\overline{f}(\mathbf{x}_i, \theta) = F_{Y_i}(\theta) = \mathbb{P}(Y_i \leq \theta)$, where $D \subseteq \mathbb{R}^d$, $\mathbf{x}_i \in G$ with its respective random variable Y_i, $\theta \in \mathbb{R}$ and F_{Y_i} the marginal CDF of Y_i. This construction is similar to the one by Kao et al. [14]. While they use an estimation of the marginal PDF, we use the marginal EDF instead. Due to the similarities to the function graph and height fields, we will refer to $\overline{f}$ as *cumulative function graph (CFG)* for the 1D case and *cumulative height field (CHF)* for 2D fields, respectively.

In practice, it is necessary to estimate the CDF and sample the range of f for each sample point. The sampling can be done uniformly, taking the global minima and maxima over all ensemble members' values as the range, introducing a parameter for the number of samples.

4.2 Visualization

Visualizing the CFG and CHF can be done through colormapping or DVR, respectively, or through isocontouring. An isocontour for the isovalue p passes through the point $(\mathbf{x}_i, \theta)$ if $F_{Y_i}(\theta) = p$. For $p = 0.5$, the isocontours would show the pointwise median, for $p = 0.25$ the first quartile, and so on. Though isolines can be adequately shown for the CFGs, isosurfaces would suffer from occlusion in the 3D case.

An important characteristic for the CFG and CHF is that all points below the pointwise sample minimum and above the sample maxima have a cumulative probability of 0 and 1, respectively. All the other points' cumulative probability values lie in the $(0,1)$ interval. Thus, colormapping CFG results usually in large segments of the same color for the points with cumulative probability 0 and 1. Hence, assigning colors to the $(0,1)$ interval is a more interesting task. Fig. 2 shows different colormappings for a synthetic 1D dataset, which also shows the members as blue line graphs. The color scales that map the estimated cumulative probability symmetrically to lightness or transparency ((c) and (d)) are better at conveying quantiles than a simple linear mapping ((a) and (b)). While both (c) and (d) show better the central quantiles, the 2D color scale in (d) maps the original codomain values to color to get a better correspondence between codomain values and cumulative probabilities. Using a divergent color scale also shows if part of the distribution are above or below some value of interest.

Using DVR for the CHF presents the typical challenges: design of a useful *transfer function* (TF), occlusion, bad depth perception and a difficult correspondence between the volume and original domain points. Regarding the TF design, it is important to choose a good opacity mapping, as the subvolumes with the cumulative probability 0 and 1 can cause occlusion, thus it is necessary to give either one, or both a low opacity. Fig. 3 shows different DVR of different TFs, analogously to Fig. 2, but using our climate dataset. In (a) and (b), the opacity decreases linearly, where for the cumulative probability of 0 and 1 the opacity is maximal and minimal, respectively. Both images show the peaks rather well, but it is difficult to see where the central quantiles are. On the other side, (c) and (d) show a symmetric opacity mapping, with the value 0.5 having opacity 0.75, and opacity 0 for both the cumulative probabilities of 0 and 1. The renderings using this opacity mapping form a "cloud" around the median, thus emphasising the median and the central quantiles. In general, it is as well possible to include shading or other methods to improve the quality and depth perception of DVR.

To improve the correspondence between the volume and the codomain values, the rendering in (d) uses a 2D TF, analogously to Fig. 2 (d), and also similar to the 2D TFs of Djurcilov et al. [9]. This 2D TF maps cumulative probability to opacity and codomain value to color. The opacity mapping is the median emphasis mapping from (c) and the colormapping can be done as in Fig. 2 (d), where the neutral color (white) is mapped to a reference value and the diverging colors are mapped to a given minimal and maximal value. Using this 2D TF provides a quick overview of where the central quantiles are above or below the reference function value.

One of the difficulties in 3D visualizations is occlusion. The use of multiple (orthographic) views from different perspectives, typically one from above and two from the sides, provides a better overview of complex scenes without having to first interact with the volume. The volume rendering of CHF is rather qualitative, giving first a general overview, and possibly helpful for the exploration of the data. A typical next step would be to deliver details for specific points or regions of interest. This selection could be made based on the top view of the data, as this view shows the original domain. However, both side views are in this case probably not useful, as the point of interest can be occluded or just cannot be clearly seen. To better examine the point of interest, we instead use the side views to show a cross section containing the point of interest and fade out the rest, e.g. through using a plane to get a subset of the data, which would actually correspond to the 1D case, the CFG. These additional cross sections enable a quantitative joint analysis of the EDF and corresponding codomain values. Kao et al. [14] uses as well cross sections to show the estimated PDF values, but they show them inside the 3D volume, while we use additional views to show them.

5 Results & Discussion

To test our method, we used the Max Planck Institute Grand Ensemble (MPI-GE) [16]. The MPI-GE includes ensemble simulations of three future scenarios: RCP2.6, RCP4.5, and RCP8.5, which describe greenhouse gas emissions due to different socio-economic developments, along with a historical simulation, a pre-industrial control run and a 1% CO_2-increase experiment. The RCP ensembles consist of 100 members each, with monthly data from January 2006 to December 2099 on a geo-referenced rectilinear 2D grid.

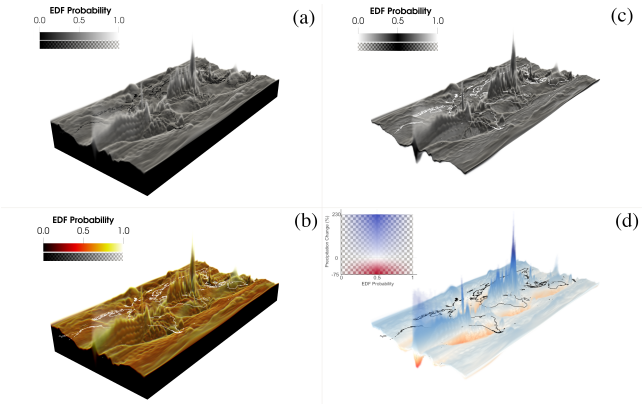

Figure 3: Comparison of different TFs on the visual appearance of volume rendering the CHF of the precipitation change (%) for 2080-2099 relative to 1986-2005 for scenario RCP8.5 as simulated within the MPI-GE ensemble: (a) the "foggy landscape", (b) "desert landscape" with black body radiation, (c) symmetric median emphasis, and (d) a 2D TF with emphasis on the median, and an isosurface of the median.

As changes in precipitation can be critical for our living conditions, we chose to focus on this variable. In particular, we looked at the relative change of yearly precipitation over time as well as at the different developments simulated for the different RCP scenarios.

In order to reduce the high-frequent noise caused by natural climate variability, we first calculated 20-year running means for each ensemble member. As a baseline, we used the ensemble mean of the 20-year mean from 1986–2005 of the yearly precipitation from the historical simulation. For each time step of each scenario, we calculated the percentage change in precipitation relative to the baseline. This ensemble of percentage change data was then used to estimate the pointwise EDF and then compute the CHF, where 700 uniformly-spaced samples were used to sample the value range of -100% to 600%. The sampled CHF was computed through an own implementation.

The resulting CHFs were visualized using DVR in ParaView [2]. To achieve better depth perception, we intended to apply DVR using the scattering model introduced in ParaView 5.11, but while this enhanced rendering worked well with simple transfer functions (TFs), it was not as successful with 2D TFs. However, to nevertheless enhance the depth perception for the 2D TFs emphasizing the median, we additionally rendered an isosurface for a cumulative probability of 0.5 (median), which provides additional visual hints. To provide the geographic context, continental outlines rendered as black lines were placed in the volume in the plane for the function value 0%. To visualize the changes over time, the volume renderings of all consecutive time step are shown as an animation, which can be found in the supplemental material.

We used a 2D TF to render the results (Fig. 4 and Fig. 1 (top left and bottom right)), which emphasizes the median as described in Sec. 4.2 and shows what parts of the distribution are above or below a value of reference. In this case, the value of reference is 0%, hence showing if the precipitation change is negative (red), zero (white), or positive (blue). The value range for the colormapping goes from -75% to 230%, respectively.

This 2D TF allows a quick overview of positive and negative changes without having to refer to a data axis. Blue-shaded maxima indicate a precipitation increase, while red-shaded depressions show areas with reduced precipitation. Regions with a thin but dense cloud indicate low variability, while more transparent vertical structures indicate high uncertainty, such as the semi-transparent bluish peaks in the tropics, which can be interpreted as regions with significant precipitation increase but with a large spread within the ensemble.

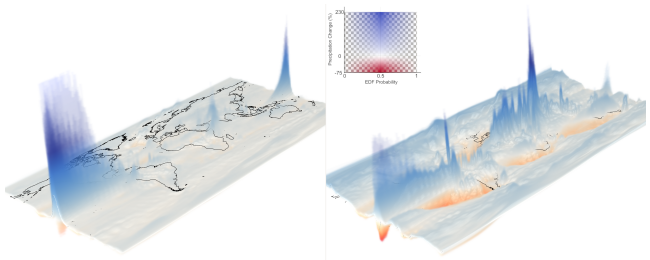

Figure 4: Overview of the precipitation change (%) for 2080-2099 relative to 1986–2005 for scenarios RCP2.6 (left) and RCP8.5 (right) as simulated within the MPI-GE ensemble, shown through volume rendering of the CHF and an isosurface of the median.

The side-by-side comparison of the precipitation change for the optimistic scenario RCP2.6 (left) and the pessimistic RCP8.5 (right) in Fig. 4 shows the differently strong patterns simulated for the end of the century: except for the blueish peaks in the tropical Pacific, RCP2.6 is rendered as an almost flat grey surface, showing that the median precipitation changes are small. The rendering of the RCP8.5 precipitation change (right) is characterized by pronounced "blue hills" and "red valleys" that resemble much stronger changes.

In addition to the perspective view of the CHF rendering (top left), Fig. 1 shows three further views that together enable a more quantitative visual analysis of the uncertain precipitation changes for RCP8.5 by the end of the century. The top view (bottom right) shows the location and intersection of two thick black lines, i.e. the positions of two cross sections through the CHF volume. The other two views show the CFG for the latitudinal cross section (bottom left) and the longitudinal one (top right).

Around the intersection of the two cross sections of Fig. 1, the width of the graded shading reflects the extremely high variability of the simulated precipitation changes in this area. The various ensemble members are uncertain here; as can be seen from the cross sections and the CFGs, both negative and positive precipitation changes are simulated within the ensemble.

6 Conclusion & Future Work

We present a novel visualization for 2D scalar field ensembles, the cumulative height fields (CHF), which gives the user a qualitative overview over all the function values and its uncertainties, similar to height fields. Due to the use of DVR, the visualization can be tweaked with the TF to highlight specific aspects of the data uncertainties, like sample minima and maxima, or the median. Some TFs were described and utilized to test the CHF with a climate ensemble, the MPI-GE. The main benefit of the visualization of the CHFs with multiple views and interaction is that it is possible to convey information about the field values and their cumulative probabilities within the ensemble simultaneously. This can also convey a fast insight about some features, e.g. high spread and skewness.

In the future, there are three main tasks we would like to address: (1) Use the CHFs with other datasets to observe further benefits and drawbacks (2) Compare the CHFs to other methods, e.g. visualization of mean with standard deviation and (3) DVR presents some challenges, like bad depth perception and occlusion, which we tried to improve using classical methods, such as multiple views, interaction and shading. We would like to further improve the correspondence between volume and original domain points, as this is relevant for a better understanding of the data. Further, it would be interesting to investigate the utility of the CHFs if other "probability functions" were used, e.g. instead of the EDF/CDF the PDF [14] or even the level crossing probabilities [21].

Acknowledgments

The authors wish to thank the Deutsche Forschungsgemeinschaft for funding the project SCHE 663/11-2.

References

[1] R. Adler and J. Taylor. *Random Fields and Geometry*. Springer Monographs in Mathematics. Springer New York, 2010. doi: 10.1007/978-0-387-48116-6 2

[2] J. Ahrens, B. Geveci, and C. Law. ParaView: An end-user tool for large data visualization. In C. D. Hansen and C. R. Johnson, eds., *Visualization Handbook*, pp. 717–731. Elesvier, 2005. doi: 10.1016/B978-012387582-2/50038-1 4

[3] R. S. Allendes Osorio and K. W. Brodlie. Contouring with Uncertainty. In I. S. Lim and W. Tang, eds., *Theory and Practice of Computer Graphics*, pp. 59–65. The Eurographics Association, 2008. doi: 10.2312/LocalChapterEvents/TPCG/TPCG08/059-065 2

[4] T. Athawale and A. Entezari. Uncertainty quantification in linear interpolation for isosurface extraction. *IEEE Transactions on Visualization and Computer Graphics*, 19:2723–32, Dec. 2013. doi: 10.1109/TVCG.2013.208 2

[5] T. Athawale, E. Sakhaee, and A. Entezari. Isosurface visualization of data with nonparametric models for uncertainty. *IEEE Transactions on Visualization and Computer Graphics*, 22(1):777–786, Jan. 2016. doi: 10.1109/TVCG.2015.2467958 2

[6] T. M. Athawale, B. Ma, E. Sakhaee, C. R. Johnson, and A. Entezari. Direct volume rendering with nonparametric models of uncertainty. *IEEE Transactions on Visualization and Computer Graphics*, 27(2):1797–1807, Feb. 2021. doi: 10.1109/TVCG.2020.3030394 2

[7] N. F. Chaves-de Plaza, P. Mody, M. Staring, R. van Egmond, A. Vilanova, and K. Hildebrandt. Inclusion depth for contour ensembles. *IEEE Transactions on Visualization and Computer Graphics*, 2024. To appear. doi: 10.1109/TVCG.2024.3350076 2

[8] N. Chaves-de-Plaza, M. Molenaar, P. Mody, M. Staring, R. Van Egmond, E. Eisemann, A. Vilanova, and K. Hildebrandt. Depth for multi-modal contour ensembles. *Computer Graphics Forum*, 43(3):e15083, June 2024. doi: 10.1111/cgf.15083 2

[9] S. Djurcilov, K. Kim, P. Lermusiaux, and A. Pang. Visualizing scalar volumetric data with uncertainty. *Computers & Graphics*, 26(2):239–248, Apr. 2002. doi: 10.1016/S0097-8493(02)00055-9 2, 3

[10] F. Ferstl, M. Kanzler, M. Rautenhaus, and R. Westermann. Visual analysis of spatial variability and global correlations in ensembles of iso-contours. *Computer Graphics Forum*, 35(3):221–230, 2016. doi: 10.1111/cgf.12898 2

[11] M. G. Genton, C. Johnson, K. Potter, G. Stenchikov, and Y. Sun. Surface boxplots. *Stat*, 3(1):1–11, 2014. doi: 10.1002/sta4.39 2

[12] M. Han, T. M. Athawale, D. Pugmire, and C. R. Johnson. Accelerated probabilistic marching cubes by deep learning for time-varying scalar ensembles. In *2022 IEEE Visualization and Visual Analytics (VIS)*, pp. 155–159, Oct. 2022. doi: 10.1109/VIS54862.2022.00040 2

[13] T. Höllt, A. Magdy, P. Zhan, G. Chen, G. Gopalakrishnan, I. Hoteit, C. D. Hansen, and M. Hadwiger. Ovis: A framework for visual analysis of ocean forecast ensembles. *IEEE Transactions on Visualization and Computer Graphics*, 20(8):1114–1126, Aug. 2014. doi: 10.1109/TVCG.2014.2307892 2

[14] D. Kao, A. Luo, J. L. Dungan, and A. Pang. Visualizing spatially varying distribution data. In *Proceedings Sixth International Conference on Information Visualisation*, pp. 219–225, July 2002. doi: 10.1109/IV.2002.1028780 2, 3, 4

[15] A. Kumpf, B. Tost, M. Baumgart, M. Riemer, R. Westermann, and M. Rautenhaus. Visualizing confidence in cluster-based ensemble weather forecast analyses. *IEEE Transactions on Visualization and Computer Graphics*, 24(1):109–119, Jan. 2018. doi: 10.1109/TVCG.2017.2745178 2

[16] N. Maher, S. Milinski, L. Suarez-Gutierrez, M. Botzet, M. Dobrynin, L. Kornblueh, J. Kröger, Y. Takano, R. Ghosh, C. Hedemann, C. Li, H. Li, E. Manzini, D. Notz, D. Putrasahan, L. Boysen, M. Claussen, T. Ilyina, D. Olonscheck, T. Raddatz, B. Stevens, and J. Marotzke. The Max Planck Institute Grand Ensemble: Enabling the exploration of climate system variability. *Journal of Advances in Modeling Earth Systems*, 11(7):2050–2069, 2019. doi: 10.1029/2019MS001639 3

[17] M. Mirzargar, R. T. Whitaker, and R. M. Kirby. Curve boxplot: Generalization of boxplot for ensembles of curves. *IEEE Transactions on Visualization and Computer Graphics*, 20(12):2654–2663, Dec. 2014. doi: 10.1109/TVCG.2014.2346455 2

[18] T. Pfaffelmoser, M. Reitinger, and R. Westermann. Visualizing the positional and geometrical variability of isosurfaces in uncertain scalar fields. *Computer Graphics Forum*, 30(3):951–960, 2011. doi: 10.1111/j.1467-8659.2011.01944.x 2

[19] T. Pfaffelmoser and R. Westermann. Visualization of global correlation structures in uncertain 2D scalar fields. *Computer Graphics Forum*, 31(3pt2):1025–1034, 2012. doi: 10.1111/j.1467-8659.2012.03095.x 2

[20] K. Potter, A. Wilson, P.-T. Bremer, D. Williams, C. Doutriaux, V. Pascucci, and C. R. Johnson. Ensemble-Vis: A framework for the statistical visualization of ensemble data. In *2009 IEEE International Conference on Data Mining Workshops*, pp. 233–240, Dec. 2009. doi: 10.1109/ICDMW.2009.55 2

[21] K. Pöthkow and H.-C. Hege. Positional uncertainty of isocontours: Condition analysis and probabilistic measures. *IEEE Transactions on Visualization and Computer Graphics*, 17(10):1393–1406, Oct. 2011. doi: 10.1109/TVCG.2010.247 2, 4

[22] K. Pöthkow and H.-C. Hege. Nonparametric models for uncertainty visualization. *Computer Graphics Forum*, 32(3pt2):131–140, 2013. doi: 10.1111/cgf.12100 2

[23] K. Pöthkow, C. Petz, and H.-C. Hege. Approximate level-crossing probabilities for interactive visualization of uncertain isocontours. *International Journal for Uncertainty Quantification*, 3(2):101–117, 2013. doi: 10.1615/Int.J.UncertaintyQuantification.2012003958 2

[24] K. Pöthkow, B. Weber, and H.-C. Hege. Probabilistic marching cubes. *Computer Graphics Forum*, 30(3):931–940, 2011. doi: 10.1111/j.1467-8659.2011.01942.x 2

[25] M. Rautenhaus, M. Böttinger, S. Siemen, R. Hoffman, R. M. Kirby, M. Mirzargar, N. Röber, and R. Westermann. Visualization in meteorology—a survey of techniques and tools for data analysis tasks. *IEEE Transactions on Visualization and Computer Graphics*, 24(12):3268–3296, 2018. doi: 10.1109/TVCG.2017.2779501 2

[26] E. Sakhaee and A. Entezari. A statistical direct volume rendering framework for visualization of uncertain data. *IEEE Transactions on Visualization and Computer Graphics*, 23(12):2509–2520, Dec. 2017. doi: 10.1109/TVCG.2016.2637333 2

[27] J. Sanyal, S. Zhang, J. Dyer, A. Mercer, P. Amburn, and R. Moorhead. Noodles: A tool for visualization of numerical weather model ensemble uncertainty. *IEEE Transactions on Visualization and Computer Graphics*, 16(6):1421–1430, Nov. 2010. doi: 10.1109/TVCG.2010.181 2

[28] B. Silverman. *Density Estimation for Statistics and Data Analysis*. Routledge, 1998. doi: 10.1201/9781315140919 2

[29] Y. Sun and M. G. Genton. Functional boxplots. *Journal of Computational and Graphical Statistics*, 20(2):316–334, Jan. 2011. doi: 10.1198/jcgs.2011.09224 2

[30] J. Wang, S. Hazarika, C. Li, and H. Shen. Visualization and visual analysis of ensemble data: A survey. *IEEE Transactions on Visualization and Computer Graphics*, 25(9):2853–2872, Sept. 2019. doi: 10.1109/TVCG.2018.2853721 2

[31] L. Wasserman. *All of Statistics: A Concise Course in Statistical Inference*. Springer New York, 2003. doi: 10.1007/978-0-387-21736-9 2

[32] R. T. Whitaker, M. Mirzargar, and R. M. Kirby. Contour boxplots: A method for characterizing uncertainty in feature sets from simulation ensembles. *IEEE Transactions on Visualization and Computer Graphics*, 19(12):2713–2722, Dec. 2013. doi: 10.1109/TVCG.2013.143 1, 2

[33] M. Zhang, Q. Li, L. Chen, X. Yuan, and J. Yong. EnConVis: A unified framework for ensemble contour visualization. *IEEE Transactions on Visualization and Computer Graphics*, 29(4):2067–2079, Apr. 2023. doi: 10.1109/TVCG.2021.3140153 2